Training in Cortically Blinded Fields Appears to Confer Patient-Specific Benefit Against Retinal Thinning

Berkeley K. Fahrenthold,[1] Matthew R. Cavanaugh,[1] Madhura Tamhankar,[2] Byron L. Lam,[3] Steven E. Feldon,[1] Brent A. Johnson,[4] and Krystel R. Huxlin[1]

[1]Flaum Eye Institute and Center for Visual Science, University of Rochester, Rochester, New York, United States
[2]Scheie Eye Institute, University of Pennsylvania, Philadelphia, Pennsylvania, United States
[3]Bascom Palmer Eye Institute, University of Miami, Miami, Florida, United States
[4]Department of Biostatistics and Computational Biology, University of Rochester, Rochester, New York, United States

Correspondence: Krystel R. Huxlin, Flaum Eye Institute, University of Rochester Medical Center, 601 Elmwood Avenue, Box 314, Rochester, NY 14642, USA; khuxlin@ur.rochester.edu.

Received: July 21, 2023
Accepted: March 6, 2024
Published: April 18, 2024

Citation: Fahrenthold BK, Cavanaugh MR, Tamhankar M, et al. Training in cortically blinded fields appears to confer patient-specific benefit against retinal thinning. *Invest Ophthalmol Vis Sci.* 2024;65(4):29. https://doi.org/10.1167/iovs.65.4.29

Purpose. Damage to the adult primary visual cortex (V1) causes vision loss in the contralateral hemifield, initiating a process of transsynaptic retrograde degeneration (TRD). Here, we examined retinal correlates of TRD using a new metric to account for global changes in inner retinal thickness and asked if perceptual training in the intact or blind field impacts its progression.

Methods. We performed a meta-analysis of optical coherence tomography data in 48 participants with unilateral V1 stroke and homonymous visual defects who completed clinical trial NCT03350919. After measuring the thickness of the macular ganglion cell and inner plexiform layer (GCL-IPL) and the peripapillary retinal nerve fiber layer (RNFL), we computed individual laterality indices (LI) at baseline and after ~6 months of daily motion discrimination training in the intact or blind field. Increasingly positive LI denoted greater layer thinning in retinal regions affected versus unaffected by the cortical damage.

Results. Pretraining, the affected GCL-IPL and RNFL were thinner than their unaffected counterparts, generating LI values positively correlated with time since stroke. Participants trained in their intact field exhibited increased $LI_{GCL\text{-}IPL}$. Those trained in their blind field had no significant change in $LI_{GCL\text{-}IPL}$. LI_{RNFL} did not change in either group.

Conclusions. Relative shrinkage of the affected versus unaffected macular GCL-IPL can be reliably measured at an individual level and increases with time post-V1 stroke. Relative thinning progressed during intact-field training but appeared to be halted by training within the blind field, suggesting a potentially neuroprotective effect of this simple behavioral intervention.

Keywords: hemianopia, quadrantanopia, vision restoration, retinal ganglion cells, automated perimetry

Cortical blindness (CB) following unilateral damage to the primary visual cortex (V1) or its immediate afferents presents as a homonymous, contralesional visual field defect. Although partial recovery can occur spontaneously in the first few months after damage,[1–4] there are no widely accepted, validated treatments for the resulting visual defect.[5] Standard of care remains "no intervention," although occasionally, patients are prescribed compensatory (e.g., saccadic) training or substitution (e.g., prism lenses) therapies.[6–9] Research also continues to show that visual perceptual training can partially restore vision in CB, measurable by both clinical perimetry and psychophysical tests of visual performance.[10–21]

The importance of developing some form of restorative therapy for CB is further highlighted by burgeoning evidence that once patients reach the chronic stage of >6 months poststroke, visual field defects do not remain completely stable, as was initially thought.[22] Instead, there appears to be progressive worsening of the perimetrically defined blind field (BF) without intervention.[11,19,22,23] The most plausible explanation for such deterioration of the BF over time is transsynaptic retrograde degeneration (TRD), which involves the progressive shrinkage and even die-back of neurons in the early visual pathways.[24–31] In humans, structural magnetic resonance imaging (MRI) analyses have shown that the optic tract ipsilateral to occipital cortex damage is often reduced in size,[25,29,30,32–35] as are the thicknesses of the ganglion cell and nerve fiber layers in corresponding regions of the retina in each eye.[24,28–32,34,36–45]

Retinal ganglion cells (RGCs) are responsible for preprocessing and ferrying visual information to the rest of the visual system. As such, their loss or dysfunction could significantly threaten the potential to recover visual functions in participants with primary visual cortex (V1) damage. Specifically, retinal neurons in the therapeutically targetable retinogeniculo-striate pathways are susceptible to TRD after occipital stroke. Isolating specific consequences of TRD in retinal regions known to synapse with V1 lesion-projecting neurons in the lateral geniculate nucleus is crucial to better under-

stand the relationship between TRD and visual retraining. Approaches to retrain the visual deficit have been shown to confer perimetrically computed improvements to CB visual fields.[16,46] However, most literature has focused on benefits to visual perception resulting from visual retraining, with limited knowledge of the effects of training on anatomic substrates of vision.[16,46] If visual training strengthens existing circuitry or recruits neuronal neighbors, similar to rehabilitation for motor stroke,[47–49] this could potentially impact retinal cells that provide input to residual visual pathways. As such, the present study asked two questions: (1) what is the extent and time course of relative thinning in affected versus unaffected inner retinal layers in humans with unilateral occipital strokes, and (2) does the stimulation afforded by visual training impact the progression of inner retinal thinning in such stroke patients? To answer these questions, we performed a meta-analysis of optical coherence tomography (OCT) data collected as part of a recently completed, multicenter, randomized, double-masked, clinical trial titled the "Hemianopia Intervention Study" (HIS; ClinicalTrials.gov identifier, NCT03350919). The HIS clinical trial design and results have been published in detail,[50] but in brief, the trial involved two pretraining clinic visits to establish eligibility and measure baseline parameters, a 6-month at-home phase during which training was administered to either the intact field (IF) or BF, and one posttraining clinic visit to evaluate the effect of training. The primary outcome measure for the HIS clinical trial was change in the 24-2 Humphrey perimetric mean deviation (PMD) from baseline, with significant improvements reported for people trained in their BF and not those trained in their IF.[50] However, the trial also performed OCT imaging and collected measurements of ganglion cell and inner plexiform layer (GCL-IPL) and retinal nerve fiber layer (RNFL) thicknesses in the affected and unaffected retina of each eye in each participant at each time point. This rich data set provided us a unique opportunity to both measure the extent of TRD in this patient cohort and analyze the impact of two different visual training interventions on TRD progression.

Methods

Participants

The HIS trial (NCT03350919) recruited 48 CB participants (see Table for demographics) at three US academic medical centers: 20 at the University of Rochester's Flaum Eye Institute, 18 at the University of Pennsylvania's Scheie Eye Institute, and 8 at the University of Miami's Bascom Palmer Eye Institute. All procedures were approved by the Western Institutional Review board (WIRB#1181904) and adhered to the tenets of the Declaration of Helsinki, and all participants gave written, informed consent.

Participants were between 21 and 75 years of age, with an MRI-confirmed occipital lesion resulting in unilateral homonymous hemianopia. Additionally, their lesions had to have occurred after the age of 18 and a minimum of 90 days prior to screening. Participants were also required to reliably fixate with both eyes during psychophysical testing and clinical Humphrey perimetry, with fixation losses and false-negative and false-positive rates during perimetry of <20%. Participants were excluded from the study if they presented with any ocular or neurologic disease that would interfere with training. Concurrent use of any other form of visual therapy or of medications that would affect training were additional exclusion criteria.

HIS Clinical Trial Design and Training Intervention

As mentioned earlier, the HIS clinical trial[50] involved two pretraining clinic visits, a 6-month at-home training phase, and one posttraining clinic visit. While the primary outcome measure was change in the 24-2 Humphrey PMD from baseline to 6 months posttraining, OCT data were also collected at each study visit, followed by computerized psychophysical testing focused on instructing participants to correctly perform the training task. Once enrolled, participants were randomized to two training arms: IF or BF training in a 1:1 ratio, using a permuted block design stratified by site. Participants randomized to these training groups did not differ in age (BF trained: 56 ± 12 years, range 32–72 years; IF trained: 61 ± 9 years, range 45–74 years; unpaired *t*-test $P = 0.0990$, 95% confidence interval [CI] = –11.83 to 1.057) or time since stroke (BF trained: 41 ± 82 months, range 3–373 months; IF trained: 43 ± 72 months, range 3-338 months; unpaired *t*-test $P = 0.9096$, 95% CI = −50.37 to 44.98).

The training intervention was a 2-alternative, forced-choice (2AFC) direction discrimination task using random dot stimuli presented either inside the BF or at a corresponding location in the IF (Table, Supplementary Materials, Supplementary Fig. S1). During the home training segment, two participants withdrew and their data are not included herein. The two cohorts trained for a comparable number of days (unpaired *t*-test $P = 0.3598$, 95% CI = −43.82 to 16.27; BF trained: 101 ± 46 days; IF trained: 115 ± 51 days).

During pretraining, in-clinic assessment, participants received instructions and underwent baseline testing with the 2AFC task within their intact and blind hemifields, with fixation enforced binocularly using an Eyelink Duo Mobile eye-tracker (SR Research, Mississauga, Ontario, Canada). Training locations were selected at sites where performance first dropped to chance (50% correct) after a 1° lateral shift along the x-axis from the intact into the BF. Using the location where performance first drops to chance as a starting point affords proximity to intact circuitry, enhancing the possibility that training may recruit perilesional V1[51] and/or induce plasticity and reintegration of residual, damaged circuitry. IF training locations were selected to be mirror symmetric to those chosen for training in the BF. CB participants were then sent home to train and were asked to perform 300 trials of the 2AFC task once daily for a minimum of 5 days per week at their assigned training location. Participants trained at a single location at a time, in the IF or BF. Once performance improved sufficiently (at least 10 sessions at a threshold <25° with a standard deviation of less than 5°), the location was moved 1° laterally away from the vertical meridian. Participant performance as a result of these interventions has been published[50] and will not be repeated here in detail.

Humphrey Visual Field Testing and Analysis

Each participant's visual deficit was quantified through Humphrey visual field (HVF) perimetry, which was performed twice in both eyes during each study visit. The University of Rochester and the University of Pennsylvania used a Humphrey Field Analyzer II-i, and the University of

Table. Participant Demographics

Subject Code	Sex	Age, Y	Time Since Stroke, Mo	Affected Visual Hemifield	Training Group
CB1	M	49	32	R	Intact
CB2	F	46	13	R	Intact
CB3	M	72	20	L	Intact
CB4	M	63	61	L	Intact
CB5	M	63	43	L	Intact
CB6	M	58	105	R	Intact
CB7	F	74	338	L	Intact
CB8	M	71	10	L	Intact
CB9	M	68	6	R	Intact
CB10	M	70	4	L	Intact
CB11	M	70	58	L	Intact
CB12	F	69	16	R	Intact
CB13	F	54	24	L	Intact
CB14	M	64	130	L	Intact
CB15	M	56	13	L	Intact
CB16	M	49	63	L	Intact
CB17	M	64	8	L	Intact
CB18	F	46	15	R	Intact
CB19	M	64	20	R	Intact
CB20	M	45	5	R	Intact
CB21	M	68	3	R	Intact
CB22	M	59	4	R	Intact
CB23	M	71	6	L	Intact
CB24	M	69	60	L	Blind
CB25	F	50	38	R	Blind
CB26	F	51	18	L	Blind
CB27	M	42	15	R	Blind
CB28	M	50	373	R	Blind
CB29	M	62	5	R	Blind
CB30	M	71	47	R	Blind
CB31	M	56	8	L	Blind
CB32	M	64	47	L	Blind
CB33	M	41	11	R	Blind
CB34	M	57	4	L	Blind
CB35	F	44	10	R	Blind
CB36	M	66	105	L	Blind
CB37	M	66	36	R	Blind
CB38	M	32	5	R	Blind
CB39	F	47	5	L	Blind
CB40	F	63	3	L	Blind
CB41	M	49	14	R	Blind
CB42	M	69	3	L	Blind
CB43	M	72	6	L	Blind

F, female; L, left; M, male; R, right.

Miami used a Humphrey Field Analyzer 3 (Zeiss Humphrey Systems, Atlanta, GA, USA), with all sites using a 24-2 testing pattern. A white, size III stimulus was presented on a background with a luminance of 11.3 cd/m^2 and thresholds were calculated with the Swedish Interactive Threshold Algorithm (SITA-standard). Participants' visual acuity was corrected to 20/20 for testing, and fixation was controlled using the gaze/blind spot automatic settings. The first test was excluded in both eyes to account for potential learning effects. If the second field set was not deemed reliable or could not be completed, the first set was used instead. Participants who did not have complete, reliable pre- and posttraining visual fields were excluded from the present HVF analyses ($n = 5$); an additional two participants failed to complete training and were also removed from our analysis. Two metrics were derived from HVF tests: the perimetric mean deviation (MD) and the average luminance detection sensitivity across the entire blind hemifield of vision. The MD is calculated by the perimeter using an internal, weighted variance from age-defined normal population values to estimate the amount of vision lost across the measured visual field. In the present study, sensitivity thresholds from the blind hemifield (ST_{BF}) were additionally averaged in each eye to capture deficit-specific changes. We then took the monocular MD and ST_{BF} and averaged them to generate a binocular (OU) version of each metric, for pre- and posttraining comparisons, in order to compare with binocularly computed OCT laterality indices.

OCT Procedures and Analysis

Retinal OCT was performed using Cirrus HD machines (Carl Zeiss Meditech, Dublin, CA, USA) at each study site before and after training. A 512 × 128 Mac Cube scan was used to examine the GCL-IPL around the fovea, and 200 × 200 optic

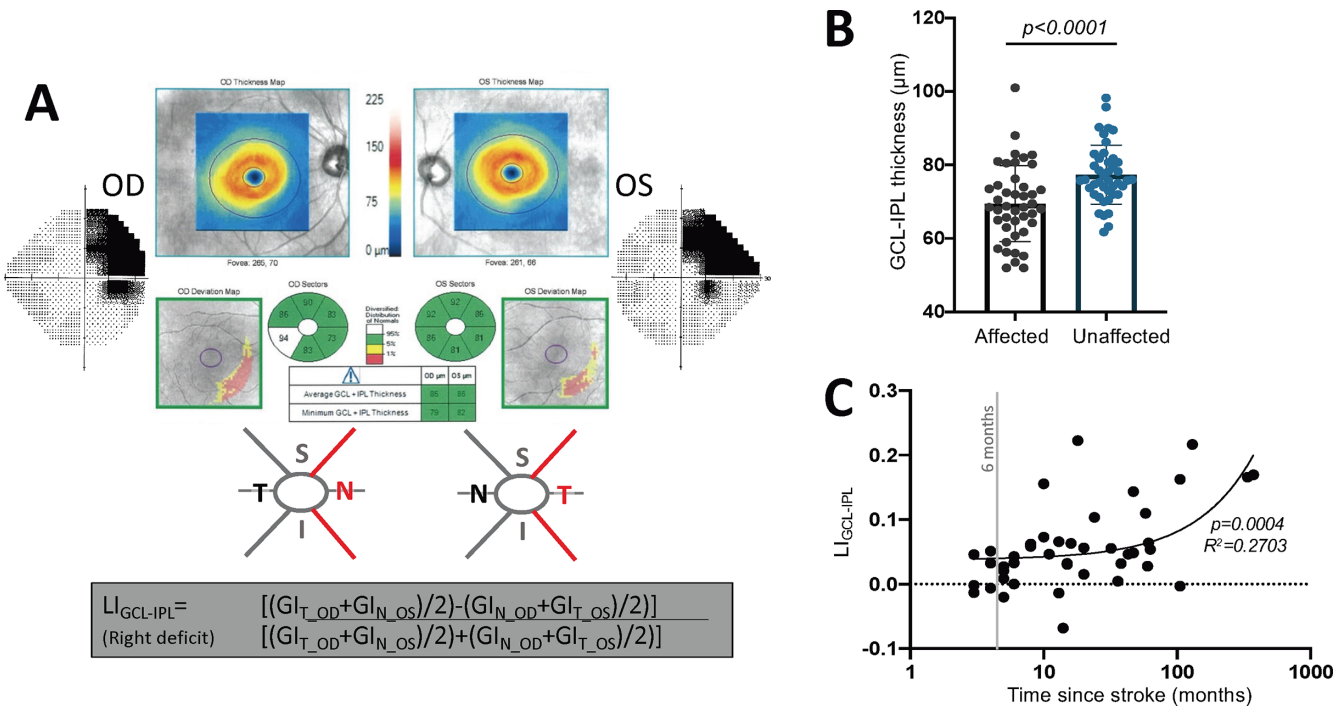

Figure 1. (**A**) Computation of LI for the GCL-IPL using the nasal (N) and temporal (T) sector GCL-IPL (GI) thickness values of both eyes, excluding superior (S) and inferior (I) sectors since they overlapped the vertical meridian. (**B**) Plot comparing GCL-IPL thicknesses in the affected or unaffected hemiretinas (paired *t*-test, 95% CI = 5.212 to 10.60, $t_{42} = 5.921$, $P = < 0.0001$). (**C**) Plot of $LI_{GCL\text{-}IPL}$ against time since stroke (linear regression, $R^2 = 0.2703$, 95% CI (y-intercept) = 0.018 to 0.057, $P = 0.0004$).

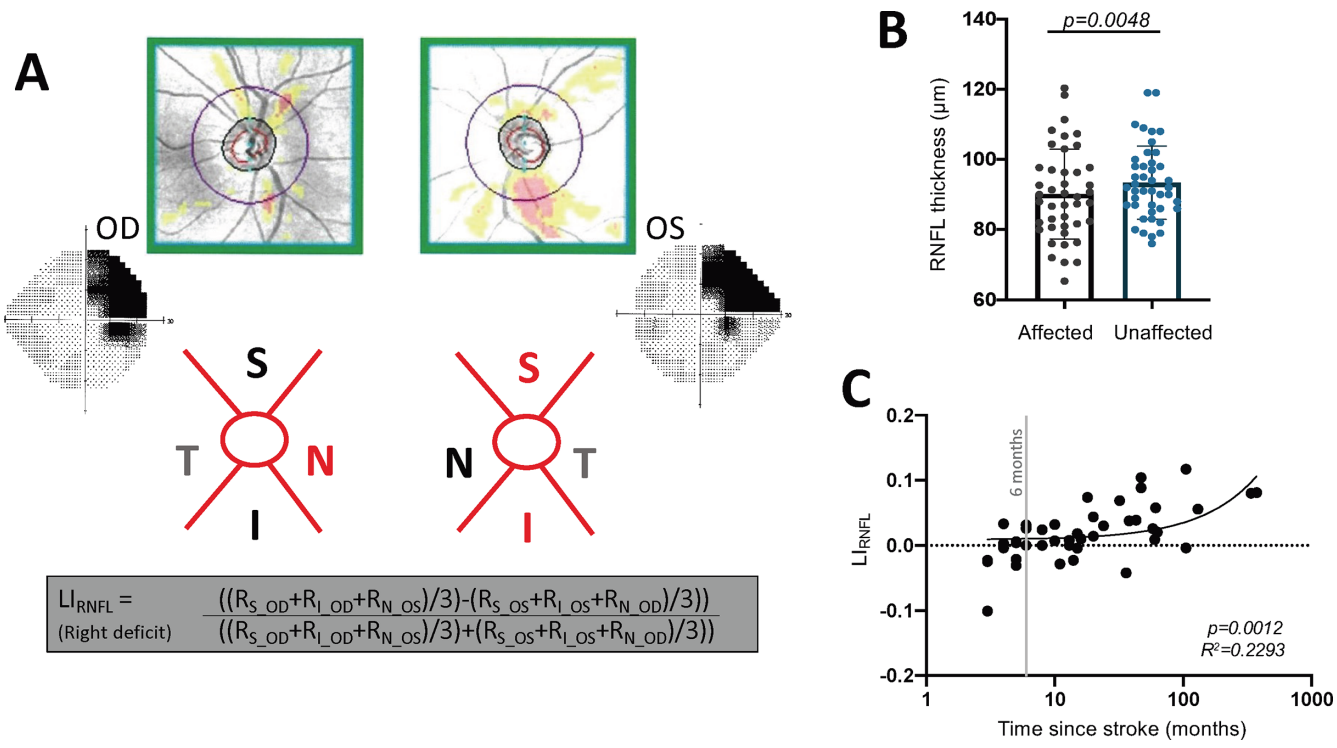

Figure 2. (**A**) Computation of LI using RNFL thickness values (R) from superior (S) and inferior (I) peripapillary regions comprising uncrossed fibers and nasal (N) peripapillary regions comprising crossed fibers representing intact or blind hemifields. (**B**) Plot comparing affected peripapillary RNFL segments carrying RGC axons representing the visual field defect to unaffected ones carrying predominantly intact field fibers (paired *t*-test, 95% CI = 1.046 to 5.450, $t_{42} = 2.977$, $P = 0.0048$). (**C**) Plot of LI_{RNFL} against time since stroke (linear regression, $R^2 = 0.2293$, 95% CI = −0.0004 to 0.0217, $P = 0.0012$).

Investigative Ophthalmology & Visual Science

nerve cube scans were used to examine the RNFL. Scans were excluded if they failed to meet signal strength ≥7 in each eye.

OCT analyses performed as part of the HIS clinical trial[50] differed from those performed here in several ways. First, they involved group-level comparisons of GCL-IPL and RNFL thickness changes pre- to posttraining across affected and unaffected retinal regions, separated by blind field sector and for each eye independently. Here, for the GCL-IPL, we combined the nasal and temporal sectors together. Furthermore, after reviewing OCT raw data, we excluded three HIS participants due to retinal folding or epiretinal membrane/RNFL detachment severe enough to impact layer thickness measurements. In remaining participants, we then computed a laterality index (LI) to account for individual, baseline thickness variances using the following formula:

$$Laterality\ \ Index = \frac{(Intact - Blind)}{(Intact + Blind)}$$

LI was computed for the GCL-IPL using the two nasal and two temporal sector values of both eyes, excluding superior and inferior sectors that overlapped the vertical meridian (Fig. 1A). The nasal and temporal macular segments of each eye corresponding to the blind or intact hemifield were then averaged together according to each participant-specific deficit. For example, a right-sided visual deficit (left-sided occipital lesion) is represented in the nasal sectors of the right eye and the temporal sectors of the left eye (see example in Fig. 1A).

Computing a laterality for the RNFL regions impacted by the deficit attempted to account for the crossed and uncrossed fibers in corresponding peripapillary sections[52] (Fig. 2A). Superior and inferior peripapillary regions comprising uncrossed fibers and nasal peripapillary regions comprising crossed fibers represent intact or blind hemifields. For example, the same right-sided visual deficit area described above was represented by the superior and inferior RNFL sectors of the left eye as well as the nasal RNFL sector of the right eye (Fig. 2A).

Statistical Analyses

Paired *t*-tests were used to assess within-subject differences. For independent sample comparisons, unpaired *t*-tests were used when contrasting two groups. If standard deviations were not the same in each group, Welch's correction was used. Linear regressions were used to model the relationship between explanatory variables and dependent outcomes, with r values and 95% CIs for ρ provided, and significance estimated using a *t*-test.

Results

Baseline Retinal Layer Thicknesses—Effects of Time Since Stroke

Prior to intervention, GCL-IPL thicknesses corresponding to the blind or intact hemifields were significantly different from each other, with the affected hemiretina's GCL-IPL being thinner than the unaffected hemiretina's (Fig. 1B). We then computed LI to factor out possible global retinal phenomena (e.g., aging related, metabolic) in order to better isolate lesion-specific degeneration in retinal regions corresponding to perimetrically defined visual deficits. The $LI_{GCL\text{-}IPL}$ was positive, averaging 0.056 ± 0.06, with a range of –0.068 to 0.29. An LI of 0 would indicate no relative thinning of the lesion-projecting compared to the non-lesion-projecting part of the retina, while positive LI values denote thinning in retinal areas representing the blind hemifield relative to those representing the intact hemifield. Importantly, the $LI_{GCL\text{-}IPL}$ was positively correlated with time since stroke (Fig. 1C), with greater thinning of the affected hemiretina GCL-IPL in participants imaged beyond 12 months poststroke compared to those imaged prior to this time point (Supplementary Fig. S2A).

A similar pattern of results was obtained for the peripapillary RNFL, which was thinner for segments carrying RGC axons representing the visual field defect compared to those carrying predominantly intact field fibers (Fig. 2B). As a result, LI_{RNFL} averaged 0.019 ± 0.04, ranging from –0.10 to 0.11. Moreover, just like $LI_{GCL\text{-}IPL}$, LI_{RNFL} was positively correlated with time since stroke (Fig. 2C), with relative thinning most pronounced beyond 12 months postlesion (Supplementary Fig. S2B). Overall, these data show clear GCL-IPL and RNFL thinning in regions of the retina carrying RGC somata, dendrites, and/or axons representing blind regions of the visual field. They also show greater thinning at later than earlier time points, especially >12 months after occipital stroke.

Effect of Visual Training on Ganglion Cell Complex Thickness

We next asked whether visual training altered signs of TRD at the level of the retina. Here, we analyzed CB patients who completed 6 months of visual training as part of the HIS clinical trial.[50] As previously reported, global direction discrimination training in the perimetrically defined BF of CB patients elicits improvements not only on the trained task but also on binocular (OU) Humphrey perimetry.[11,50] Consistent with this observation, participants trained in their BF exhibited a systematic improvement in OU MD (Fig. 3A). To ascertain if the change in MD was driven by the blind hemifield (versus improved ability to perform Humphrey perimetry across the entire test area), we also computed OU ST_{BF} change for the blind hemifield. OU ST_{BF} improved significantly following BF training (Fig. 3B), contrasting with a lack of significant changes—for both OU MD and ST_{BF}—in the IF-trained cohort (Figs. 3D, 3E). Notably, a strong correlation exists between MD and ST_{BF} in both cohorts, pre- and posttraining (Figs. 3C, 3F).

Having established a subtle but differential effect of training on perimetry between the two cohorts, we then asked if—and to what degree—the two types of interventions impacted retinal thinning. For $LI_{GCL\text{-}IPL}$, there was a significant overall increase pre- to posttraining across all participants (Fig. 4A). However, no detectable changes occurred pre- to posttraining overall in LI_{RNFL} (Fig. 4B). Separating the two interventions, $LI_{GCL\text{-}IPL}$ was significantly larger posttraining in those who trained in their intact field (Fig. 5A) but not in BF-trained participants (Fig. 5B). Furthermore, in the IF training group, raw GCL-IPL thicknesses were significantly lower in the posttraining affected hemiretina (Fig. 5C). Posttraining affected GCL-IPL thicknesses also significantly

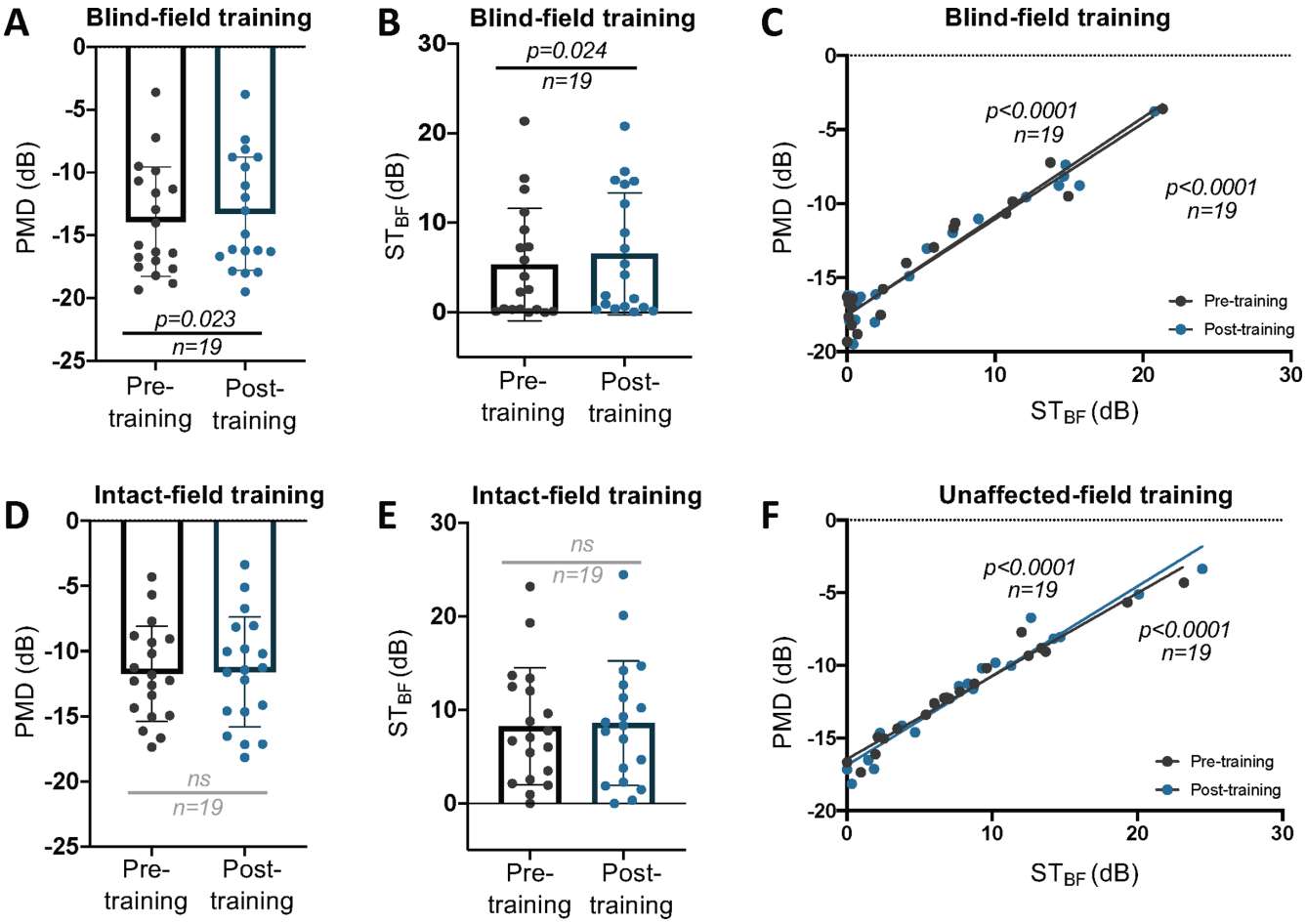

Figure 3. (**A**) Plot of pre- and posttraining OU MD in BF-trained participants (paired *t*-test, 95% CI = 0.098 to 1.2, $t_{18} = 2.473$, $P = 0.023$, mean of differences = 0.65 ± 1.15). (**B**) OU ST_{BF} pre- and posttraining following BF training (paired *t*-test, 95% CI = 0.177 to 2.258, $t_{18} = 2.458$, $P = 0.024$, mean of differences = 1.22 ± 2.16). (**C**) Linear regression of MD against ST_{BF} pretraining: $R^2 = 0.9365$, 95% CI (y-intercept) = −18.28 to −16.82; post-BF training: $P < 0.0001$; $R^2 = 0.9526$, 95% CI (y-intercept) = −18.21 to −16.84, $P < 0.0001$. (**D**) Plot of pre- and posttraining OU MD in IF-trained participants (paired *t*-test, 95% CI = −0.3284 to 0.6284, $t_{18} = 0.6587$, $P = 0.5184$, mean of differences = 1.5 ± 0.9926). (**E**) OU ST_{BF} pre- and posttraining following IF training (paired *t*-test, 95% CI = −0.1917 to 0.8655, $t_{18} = 1.339$, $P = 0.1972$, mean of differences = 0.3369 ± 1.097). (**F**) Linear regression of MD against ST_{BF} pretraining: $R^2 = 0.963$, 95% CI (y-intercept) = −17.04 to −15.87; post-IF training: $P < 0.0001$; $R^2 = 0.9481$, 95% CI (y-intercept) = −17.67 to −16.08, $P < 0.0001$). ns, not statistically significant.

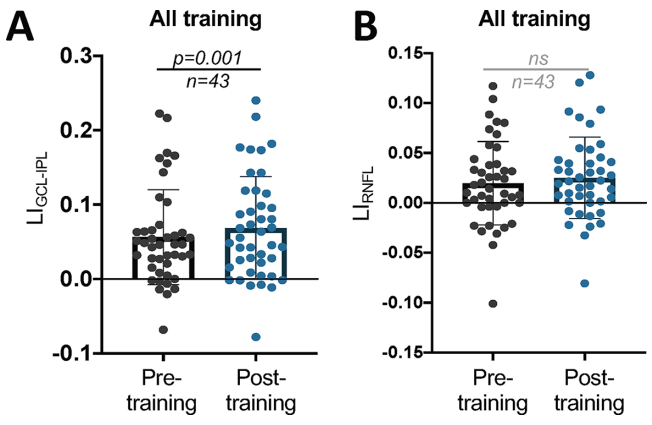

Figure 4. (**A**) Plot of $LI_{GCL-IPL}$ pre- and posttraining for all participants (paired *t*-test, 95% CI = 0.005 to 0.019, $t_{42} = 3.424$, $P = 0.001$). (**B**) Plot of LI_{RNFL} pre- and posttraining for all participants (paired *t*-test, 95% CI = −0.0015 to 0.01251, $t_{42} = 1.572$, $P = 0.1234$). ns, not statistically significant.

changed from pretraining in the BF training group (Fig. 5D). Additionally, a significant difference in magnitude of change in the affected relative to unaffected hemiretinas was present in IF-trained participants, and critically, no such difference was found in BF-trained participants (Fig. 5E). However, we fail to reject the null hypothesis that the pre–post differences of the affected hemiretinas differ by training type (Fig. 5E).

When assessing the impact of training on the RNFL, no significant change in LI_{RNFL} was found in either group pre- to posttraining (Figs. 6A, 6B). Similarly, no significant pre–post training differences were observed in either training cohort for raw RNFL thickness (Figs. 6C, 6D). Additionally, when assessing pre–post change, no significant differences were seen between or within training groups (Fig. 6E).

Consistent with these findings, changes in ST_{BF} and $LI_{GCL-IPL}$ were directly (and inversely) correlated in those trained in their blind hemifield (Fig. 7A) but not in those trained in their IF (Fig. 7B). No significant correlations were

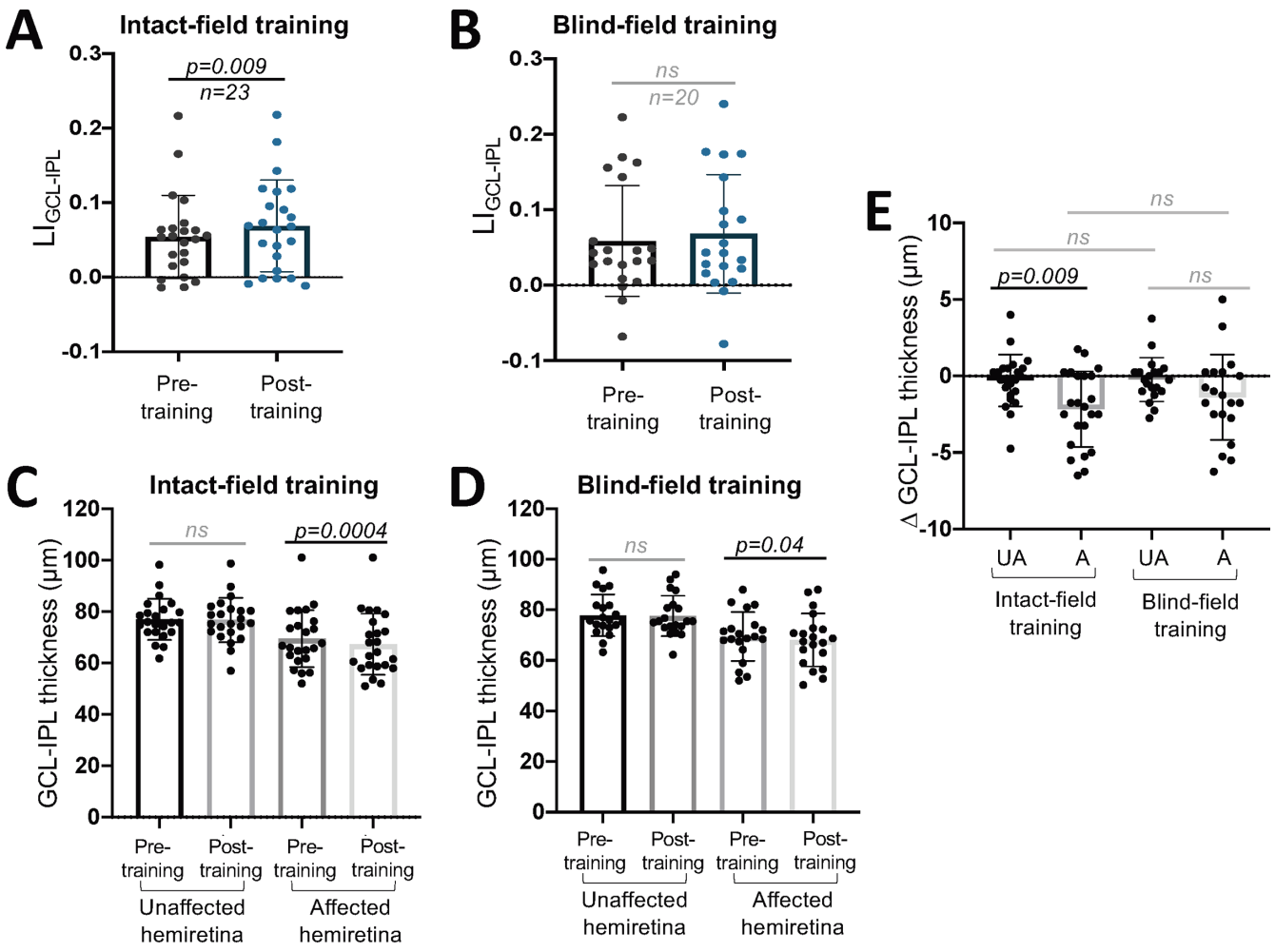

Figure 5. (**A**) Plot of $LI_{GCL\text{-}IPL}$ pre- and posttraining for participants who trained in their IF (paired *t*-test, 95% CI = 0.003 to 0.025, t_{22} = 2.837, P = 0.0096). (**B**) Plot of $LI_{GCL\text{-}IPL}$ pre- and posttraining for participants who trained in their BF (paired *t*-test, 95% CI = −0.0008 to 0.0199, t_{19} = 1.916, P = 0.07). (**C**) Comparisons of unaffected and affected hemiretina GCL-IPL thicknesses, before and after training in the IF (unaffected pre- versus posttraining: paired *t*-test, 95% CI = −1.017 to 0.4516, P = 0.4332; affected pre- versus posttraining: paired *t*-test, 95% CI = −3.233 to −1.093, P = 0.0004). (**D**) Comparison of unaffected and affected hemiretina GCL-IPL thicknesses, before and after BF training (unaffected pre- versus posttraining: paired *t*-test, 95% CI = −0.8943 to 0.4443, P = 0.4902; affected pre- versus posttraining: paired *t*-test, 95% CI = −2.691 to −0.0843, P = 0.04). (**E**) Comparison of change in GCL-IPL thickness from pre- to posttraining in IF- or BF-trained participants (unaffected versus affected hemiretina in IF-trained subjects, paired *t*-test, 95% CI = 0.2063 to 3.555, P = 0.009; unaffected versus affected hemiretina in BF-trained subjects, 95% CI = −2.601 to 0.2762, P = 0.1071; unaffected versus unaffected of both training groups, unpaired *t*-test, 95% CI = −0.9176 to 1.033, P = 0.9056; affected versus affected of both training groups, unpaired *t*-test, 95% CI = −0.8438 to 2.395, P = 0.3391). A, affected; ns, not statistically significant; UA, unaffected.

observed between changes in ST_{BF} and LI_{RNFL} in either training cohort (Figs. 7C, 7D).

Discussion

The present study asked—for the first time—whether visual stimulation provided by perceptual training alters the progression of retinal ganglion cell layer complex thinning after stroke damage to the occipital cortex in adult humans. First, we confirmed prior reports of relative thinning in the affected versus unaffected retinas' GCL-IPL and RNFL after unilateral V1 damage[28,29,31,32,34,36,39,41,53] using noninvasive OCT imaging. Second, the spread of poststroke times at participant enrollment allowed us to define a time course for this thinning. Finally, we now provide evidence that a simple behavioral intervention slows or blocks the progression of relative GCL-IPL thinning, whereas comparable stimulation of the intact hemifield of vision fails to do so.

Occipital Damage Causes Variable, Progressive Shrinkage of the Ganglion Cell Complex

Our observations showed that the largest, positive deviations from 0 in $LI_{GCL\text{-}IPL}$ and LI_{RNFL} occurred beyond 12 months poststroke. While some deviation in $LI_{GCL\text{-}IPL}$ (but not LI_{RNFL}) was also observed in our earliest participants, there was considerable interindividual variability, which precluded a significance analysis in the present cohort. Large deviations of LI values from 0 were previously observed for optic tract volumes using structural magnetic resonance imaging, starting from ~6 months poststroke, albeit also with large interindividual variability.[35] This time course differential makes some sense if one considers that the optic tract contains the distal portions of RGC axons, right before they synapse in the dorsal lateral geniculate nucleus. These distal axons, being closer to the V1 lesion site, might exhibit earlier signs of target

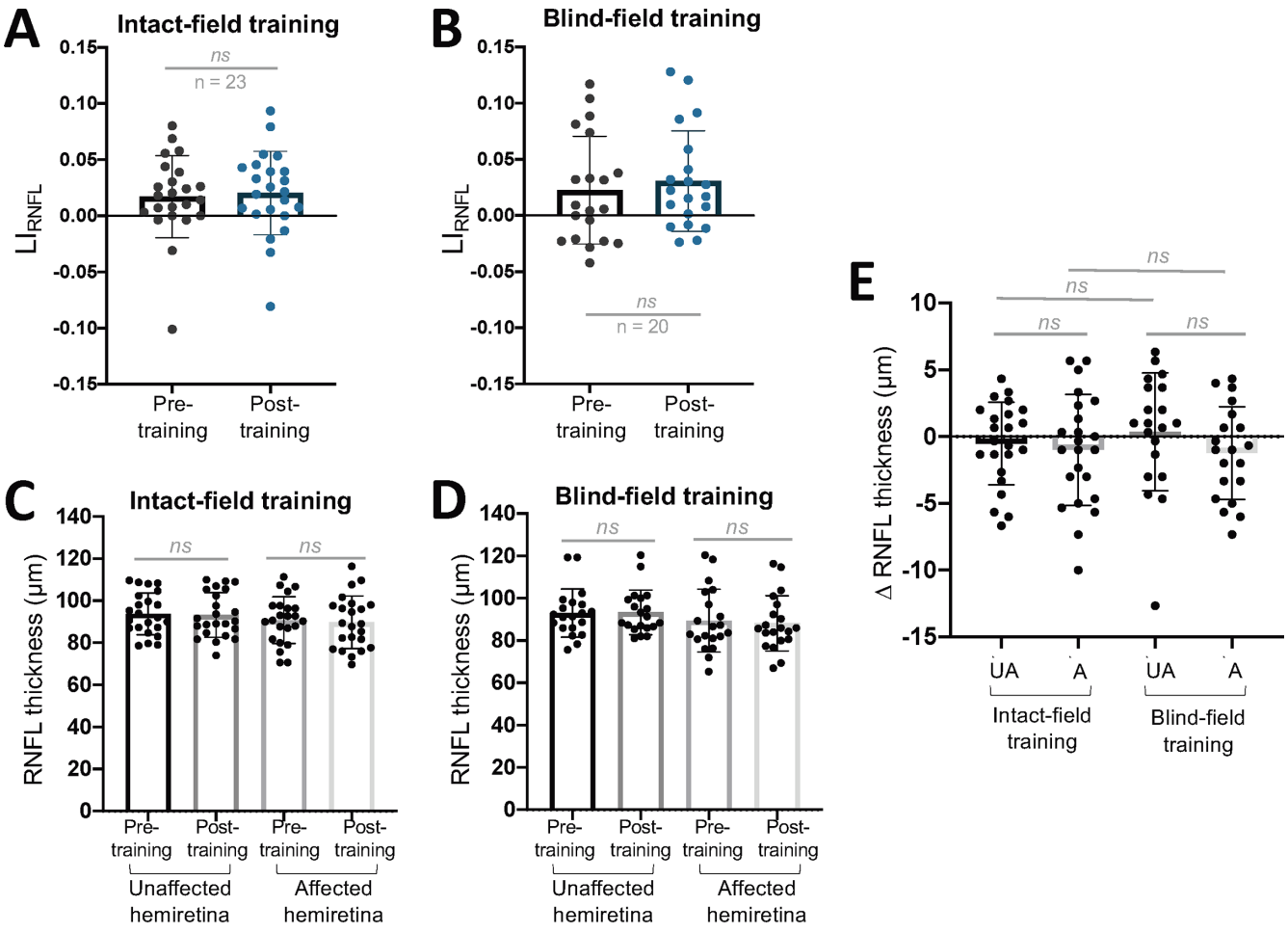

Figure 6. (**A**) Plot of LI_{RNFL} pre- and posttraining for participants who trained in their IF (paired *t*-test, 95% CI = −0.003 to 0.0123, t_{22} = 0.7322, P = 0.4718). (**B**) Plot of LI_{RNFL} pre- and posttraining for participants who trained in their BF (paired *t*-test, 95% CI = −0.0036 to 0.0197, t_{19} = 1.446, P = 0.1645). (**C**) Comparison of unaffected and affected RNFL thicknesses, before and after IF training (unaffected pre- versus posttraining: paired *t*-test, 95% CI = −1.860 to 0.8163, P = 0.4274; affected pre- versus posttraining: paired *t*-test, 95% CI = −2.796 to 0.7962, P = 0.2606). (**D**) Comparison of unaffected and affected RNFL thicknesses, before and after BF training (unaffected pre- versus posttraining: paired *t*-test, 95% CI = −1.714 to 2.414, P = 0.7266; affected pre- versus posttraining: paired *t*-test, 95% CI = −2.862 to 0.3951, P = 0.1294). (**E**) Comparison of change in RNFL thickness from pre- to posttraining in IF- or BF-trained participants (unaffected versus affected in IF-trained subjects: paired *t*-test, 95% CI = −2.096 to 1.139, P = 0.546; unaffected versus affected in BF-trained subjects: paired *t*-test, 95% CI = −3.627 to 0.4601, P = 0.1213; unaffected versus unaffected of both training groups: unpaired *t*-test, 95% CI = −1.451 to 3.195, P = 0.4529; affected versus affected of both training groups: unpaired *t*-test, 95% CI = −2.614 to 2.148, P = 0.8441). A, affected; ns, not statistically significant; UA, unaffected.

loss and degeneration than the cell bodies and dendritic arbors of the parent cells in the retina, but once again, a larger sample size earlier poststroke would be needed to make this determination from a statistically valid standpoint.

As stated earlier, a positive LI reflects a relative thinning of the lesion-projecting versus intact hemisphere–projecting portions of the macular GCL-IPL. This relative thinning could be attributable to shrinking of the RGC soma, cell death, and/or changes in cell branching; similarly, relative thinning in the RNFL could result from RGC axonal loss, shrinkage, or both.[24,28,29,32,34,37,40,53–55] Although past studies show that RGCs are ultimately lost over time after occipital damage,[28,29,31,55,56] there is also evidence that RGCs change size based on metabolic activity or the beginning stages of apoptosis.[57,58] As such, slowing or even reversing retinal thinning may be possible if intervention occurs prior to significant cell death.

Importantly, both the GCL-IPL and RNFL were previously reported to thin with increasing age in humans,[59] a fact confirmed in the present data set, and likely related to cell loss and/or shrinkage (Supplementary Fig. S3). However, it is important to note that by computing and tracking changes in LI rather than raw layer thicknesses, we were able to dissociate the impact of the occipital stroke and subsequent training interventions from this natural trend.

Visual Training May Block the Progression of Relative Ganglion Cell Complex Thinning

Despite initial retinal ganglion cell complex thinning at baseline, participants who trained in their BF for 6 months showed improvements in binocular performance metrics derived from Humphrey perimetry and seemed to avoid the increase in $LI_{GCL-IPL}$ that occurred in participants randomized to train in their IF. While GCL-IPL thickness decreased

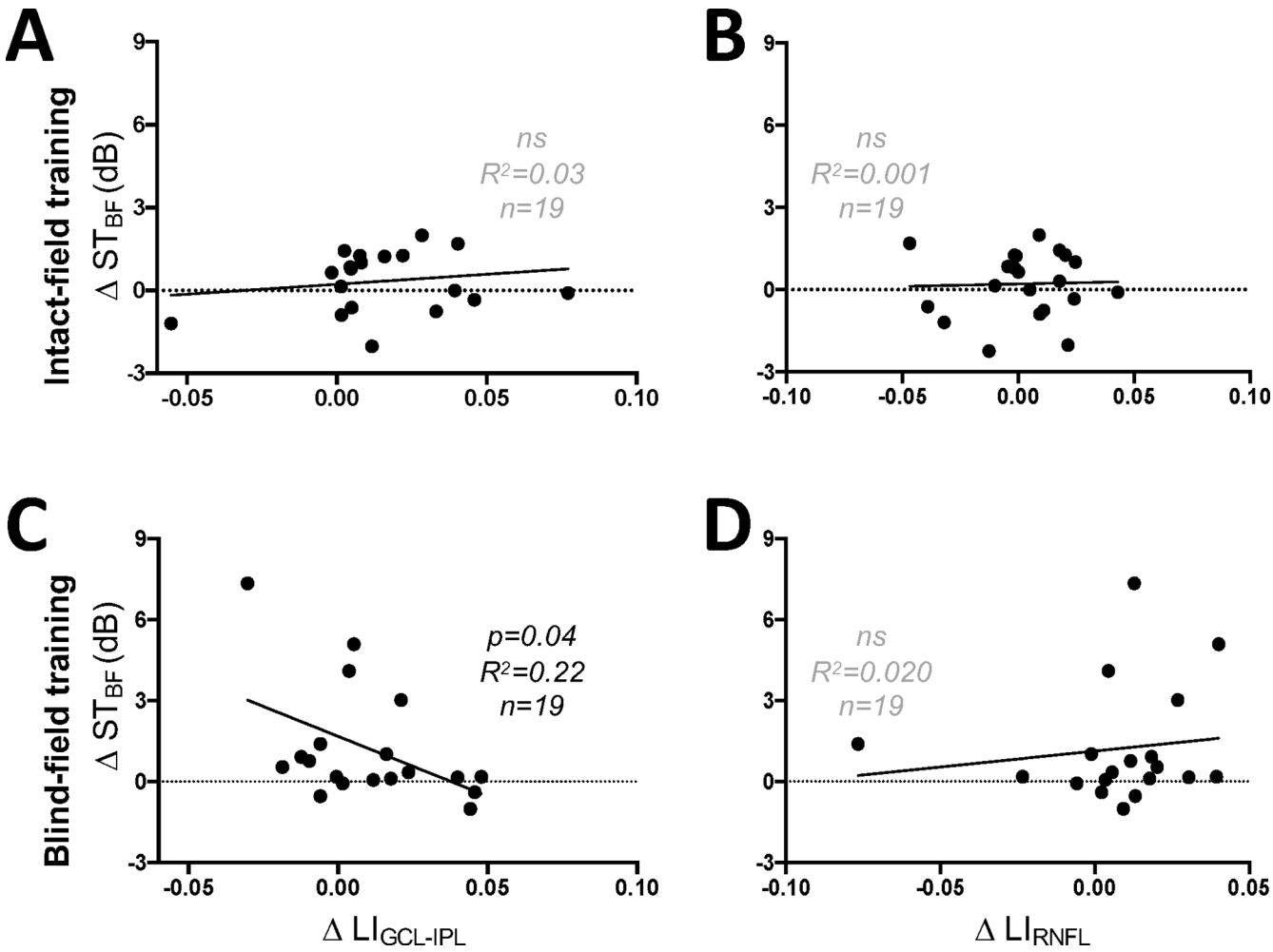

Figure 7. (**A**) Plot of change in ST_{BF} against $LI_{GCL\text{-}IPL}$ of participants trained in their IF (linear regression, $R^2 = 0.0307$, 95% CI (y-intercept) = −0.3997 to 0.8511, $P = 0.4727$). (**B**) Plot of changes in ST_{BF} and LI_{RNFL} in IF-trained participants (linear regression, $R^2 = 0.001$, 95% CI (y-intercept) = −0.3497 to 0.766, $P = 0.8857$). (**C**) Plot of change in ST_{BF} against $LI_{GCL\text{-}IPL}$ of participants trained in their BF (linear regression, $R^2 = 0.2170$, 95% CI (y-intercept) = 0.6239 to 2.723, $P = 0.04$). (**D**) Plot of changes in ST_{BF} and LI_{RNFL} in participants training in the BF (linear regression, $R^2 = 0.0196$, 95% CI (y-intercept) = 0.0093 to 2.241, $P = 0.5674$).

in both groups, the change in GCL-IPL thickness of the affected relative to the unaffected hemiretina was only significant in the IF-trained participants. Coupled with a failure to reject the null hypothesis in pre- to posttraining differences of $LI_{GCL\text{-}IPL}$ in the BF-trained group, this suggests a subtle but significant effect of training location on GCL-IPL thinning within a given patient, which is lost when comparing effects across individuals. The inherent variability in OCT layer thickness in small cohorts makes it difficult to compare groups directly. This is further complicated by variability introduced due to time-dependent TRD. In the future, increasing the sample size to increase sensitivity is crucial to better understanding the anatomic underpinnings of visual retraining. This is a difficult endeavor with two critical limitations: (1) CB participants with lesions limited to the occipital cortex are rare and challenging to recruit, and (2) once recruited, CB participants require time-intensive testing and evaluation. Alleviating these limitations would require expansion of collaborating facilities and personnel, as well as relaxing inclusion and exclusion recruitment criteria, leading to a more heterogenous patient population. However, despite current limitations, these within-group comparisons provide novel insights into training-dependent changes within the early visual pathway.

These surprising observations suggest first that OCT imaging and our derived LI metric is a sensitive biomarker for assessing the impact of training in poststroke CB patients. Just as importantly, it also suggests that an intervention that locally stimulates RGCs in a retinal area deprived of several key central targets may benefit the structural integrity of these residual cells. In turn, this may increase the likelihood that these neurons are retained long term in the residual visual circuitry, perhaps providing the neural substrates of training-induced recovery of visual functions seen deeper into the visual deficit.[51] Conversely, training within the intact field locally stimulates circuits that are not directly affected by V1 damage-mediated TRD.[26,29,43] Although V1 areas of both hemispheres representing visual information along the vertical meridian are connected via callosal axonal projections,[60] notable due to the training locations of these participants, these interhemispheric connections do not appear to provide enough benefit to the anterior portion of the visual pathway to be observable at the level of the retina.

So, what could underlie the stabilization of $LI_{GCL-IPL}$ in BF-trained participants? As mentioned earlier, damaged RGCs undergo changes in their dendritic arbors in the IPL[61,62] and in supporting cells, such as Müller glia,[57,58,63] which span the entire thickness of the retina. Training in the BF could increase the energy demands of stimulated RGCs and, by consequence, of surrounding supporting cells, in turn causing structural changes manifested as a cell-size increase and/or shrinkage prevention.[36,57] Changes in surviving RGCs are of course likely occurring in tandem with RGC loss due to retrograde degeneration—a phenomenon on which visual training's effects are unknown.

An important question emerging from the present results is whether the stabilization of the $LI_{GCL-IPL}$ persists after BF training stops. If this phenomenon relies on increased retinal activity due to training, it is possible that physiologic mechanisms of TRD will eventually overcome the benefits gained once training ceases. However, it is also possible that if participants incorporate their regained visual abilities into everyday usage, they could maintain them and sustain their associated circuits.

Finally, we saw no significant changes in LI_{RNFL} or RNFL thickness in either training cohort, although several factors likely limited our ability to detect such changes with OCT, including the anatomic complexities of the RNFL in different peripapillary zones, the very small volume of the RNFL overall, our relatively small sample size, and intersubject variability. Future studies using larger sample sizes, more detailed analyses, and better imaging resolution will be required to rigorously elucidate the impact of training on the RNFL.

Conclusions

In conclusion, the present work investigated the impact of a visual training intervention administered either inside the blind or intact field of occipital stroke patients on the progression of TRD at the level of the inner retina. We found that relative thinning in the GCL-IPL and RNFL mirrored a distinct time course poststroke previously reported in the literature. Training for ~6 months with a motion discrimination task inside the blind hemifield appeared to block the progression of relative thinning in the ganglion cell complex. In contrast, this relative thinning proceeded unabated when training was administered to the intact field of vision. Our results provide the first evidence of a greater structural benefit in the retina for a behavioral intervention that stimulates circuitry impacted by V1 damage over one that stimulates the intact circuitry.

Acknowledgments

Supported by NIH funding (R01 EY027314 to KRH, as well as T32 EY007125 and P30 EY001319 to the Center for Visual Science) and by an unrestricted grant from the Research to Prevent Blindness (RPB) Foundation to the Flaum Eye Institute. The HIS clinical trial was funded by the Center of Emerging and Innovative Science for Empire State Development (project no. 1730C004), the Center of Excellence (project no. 1689bC2), and EnVision Solutions LLC. The sponsors and funding organizations had no role in the design or conduct of this research.

Disclosure: **B.K. Fahrenthold**, None; **M.R. Cavanaugh**, None; **M. Tamhankar**, None; **B.L. Lam**, None; **S.E. Feldon**, None; **B.A. Johnson**, None; **K.R. Huxlin**, (P)

References

1. Gray CS, French JM, Bates D, Cartlidge NE, Venables GS, James OF. Recovery of visual fields in acute stroke: homonymous hemianopia associated with adverse prognosis. *Age Ageing*. 1989;18:419–421.
2. Lin S, George BZ, Wilson-Holt NJ. Perimetric demonstration of spontaneous visual field recovery following occipital lobe haemorrhage. *BMJ Case Rep*. 2013;2013:bcr2013010494.
3. Zhang X, Kedar S, Lynn MJ, Newman NJ, Biousse V. Homonymous hemianopia in stroke. *J Neuroophthalmol*. 2006;26:180.
4. Zhang X, Kedar S, Lynn MJ, Newman NJ, Biousse V. Natural history of homonymous hemianopia. *Neurology*. 2006;66:901–905.
5. Perez C, Chokron S. Rehabilitation of homonymous hemianopia: insight into blindsight. *Front Integr Neurosci*. 2014;8:82.
6. Peli E. Field expansion for homonymous hemianopia by optically induced peripheral exotropia. *Optom Vis Sci*. 2000;77:453–464.
7. Sahraie A, Smania N, Zihl J. Use of NeuroEyeCoach to improve eye movement efficacy in patients with homonymous visual field Loss. *BioMed Res Int*. 2016;2016:5186461.
8. Weinberg J, Diller L, Gordon WA, et al. Visual scanning training effect on reading-related tasks in acquired right brain damage. *Arch Phys Med Rehabil*. 1977;58:479–486.
9. Pollock A, Hazelton C, Rowe FJ, et al. Interventions for visual field defects in people with stroke. *Cochrane Database Syst Rev*. 2019;5:CD008388.
10. Bergsma DP, Elshout JA, van den Berg AV. Segregation of spontaneous and training induced recovery from visual field defects in subacute stroke patients. *Front Neurol*. 2017;8:681.
11. Cavanaugh MR, Huxlin KR. Visual discrimination training improves Humphrey perimetry in chronic cortically induced blindness. *Neurology*. 2017;88:1856–1864.
12. Cavanaugh MR, Zhang R, Melnick MD, et al. Visual recovery in cortical blindness is limited by high internal noise. *J Vis*. 2015;15:9.
13. Chokron S, Perez C, Obadia M, Gaudry I, Laloum L, Gout O. From blindsight to sight: cognitive rehabilitation of visual field defects. *Restor Neurol Neurosci*. 2008;26:305–320.
14. Das A, Tadin D, Huxlin KR. Beyond blindsight: properties of visual relearning in cortically blind fields. *J Neurosci*. 2014;34:11652–11664.
15. Huxlin KR, Martin T, Kelly K, et al. Perceptual relearning of complex visual motion after V1 damage in humans. *J Neurosci*. 2009;29:3981–3991.
16. Melnick MD, Tadin D, Huxlin KR. Relearning to see in cortical blindness. *Neuroscientist*. 2016;22:199–212.
17. Raninen A, Vanni S, Hyvärinen L, Näsänen R. Temporal sensitivity in a hemianopic visual field can be improved by long-term training using flicker stimulation. *J Neurol Neurosurg Psychiatry*. 2007;78:66–73.
18. Sahraie A, Macleod M-J, Trevethan CT, et al. Improved detection following neuro-eye therapy in patients with postgeniculate brain damage. *Exp Brain Res*. 2010;206:25–34.
19. Saionz EL, Tadin D, Melnick MD, Huxlin KR. Functional preservation and enhanced capacity for visual restoration in subacute occipital stroke. *Brain*. 2020;143:1857–1872.
20. Trevethan CT, Urquhart J, Ward R, Gentleman D, Sahraie A. Evidence for perceptual learning with repeated stimulation after partial and total cortical blindness. *Adv Cogn Psychol*. 2012;8:29–37.
21. Vaina LM, Soloviev S, Calabro FJ, Buonanno F, Passingham R, Cowey A. Reorganization of retinotopic maps after occipital lobe infarction. *J Cogn Neurosci*. 2014;26:1266–1282.

22. Wang V, Saionz E, Cavanaugh M, Huxlin K. Natural progression of perimetric visual field defects after V1 stroke. *J Vis*. 2017;17:51–52.
23. Saionz EL, Cavanaugh MR, Johnson BA, Harrington D, Aguirre GK, Huxlin KR. The natural history of homonymous hemianopia revisited. 2022. https://www.medrxiv.org/content/10.1101/2022.10.06.22280668v1. Accessed February 16, 2023.
24. Beatty R, Sadun A, Smith L, Vonsattel J, Richardson E. Direct demonstration of transsynaptic degeneration in the human visual system: a comparison of retrograde and anterograde changes. *J Neurol Neurosurg Psychiatry*. 1982;45:143–146.
25. Bridge H, Jindahra P, Barbur J, Plant GT. Imaging reveals optic tract degeneration in hemianopia. *Invest Ophthalmol Vis Sci*. 2011;52:382–388.
26. Cowey A, Stoerig P, Perry VH. Transneuronal retrograde degeneration of retinal ganglion cells after damage to striate cortex in macaque monkeys: selective loss of P beta cells. *Neuroscience*. 1989;29:65–80.
27. Cowey A, Alexander I, Stoerig P. Transneuronal retrograde degeneration of retinal ganglion cells and optic tract in hemianopic monkeys and humans. *Brain*. 2011;134:2149–2157.
28. Herro A, Lam B. Retrograde degeneration of retinal ganglion cells in homonymous hemianopsia. *Clin Ophthalmol*. 2015;9:1057–1064.
29. Jindahra P, Petrie A, Plant GT. Retrograde trans-synaptic retinal ganglion cell loss identified by optical coherence tomography. *Brain*. 2009;132:628–634.
30. Jindahra P, Petrie A, Plant GT. The time course of retrograde trans-synaptic degeneration following occipital lobe damage in humans. *Brain*. 2012;135:534–541.
31. Park H-YL, Park YG, Cho A-H, Park CK. Transneuronal retrograde degeneration of the retinal ganglion cells in patients with cerebral infarction. *Ophthalmology*. 2013;120:1292–1299.
32. Meier PG, Maeder P, Kardon RH, Borruat F-X. Homonymous ganglion cell layer thinning after isolated occipital lesion: macular OCT demonstrates transsynaptic retrograde retinal degeneration. *J Neuroophthalmol*. 2015;35(2):112–116.
33. Millington RS, Yasuda CL, Jindahra P, et al. Quantifying the pattern of optic tract degeneration in human hemianopia. *J Neurol Neurosurg Psychiatry*. 2014;85:379–386.
34. Yamashita T, Miki A, Goto K, et al. Retinal ganglion cell atrophy in homonymous hemianopia due to acquired occipital lesions observed using cirrus high-definition-OCT. *J Ophthalmol*. 2016;2016:1–9.
35. Fahrenthold BK, Cavanaugh MR, Jang S, et al. Optic tract shrinkage limits visual restoration after occipital stroke. *Stroke*. 2021;52:3642–3650.
36. Schneider CL, Prentiss EK, Busza A, et al. Survival of retinal ganglion cells after damage to the occipital lobe in humans is activity dependent. *Proc R Soc B Biol Sci*. 2019;286:9.
37. Goto K, Miki A, Yamashita T, et al. Sectoral analysis of the retinal nerve fiber layer thinning and its association with visual field loss in homonymous hemianopia caused by post-geniculate lesions using spectral-domain optical coherence tomography. *Graefes Arch Clin Exp Ophthalmol*. 2016;254:745–756.
38. Keller J, Sánchez-Dalmau BF, Villoslada P. Lesions in the posterior visual pathway promote trans-synaptic degeneration of retinal ganglion cells. *PLoS ONE*. 2014;9:e97444.
39. Mehta JS, Plant GT. Optical coherence tomography (OCT) findings in congenital/long-standing homonymous hemianopia. *Am J Ophthalmol*. 2005;140:727–729.
40. Mitchell JR, Oliveira C, Tsiouris AJ, Dinkin MJ. Corresponding ganglion cell atrophy in patients with postgeniculate homonymous visual field loss. *J Neuroophthalmol*. 2015;35:353–359.
41. Porrello G, Falsini B. Retinal ganglion cell dysfunction in humans following post-geniculate lesions: specific spatio–temporal losses revealed by pattern ERG. *Vis Res*. 1999;39:1739–1748.
42. Shin H-Y, Park H-YL, Choi J-A, Park CK. Macular ganglion cell–inner plexiform layer thinning in patients with visual field defect that respects the vertical meridian. *Graefes Arch Clin Exp Ophthalmol*. 2014;252:1501–1507.
43. Simmen CF, Fierz FC, Michels L, et al. Lateral geniculate nucleus volume determined on MRI correlates with corresponding ganglion cell layer loss in acquired human postgeniculate lesions. *Invest Ophthalmol Vis Sci*. 2022;63:18.
44. Yamashita T, Miki A, Goto K, et al. Evaluation of significance maps and the analysis of the longitudinal time course of the macular ganglion cell complex thicknesses in acquired occipital homonymous hemianopia using spectral-domain optical coherence tomography. *Neuroophthalmology*. 44:236–245.
45. Zangerl B, Whatham A, Kim J, et al. Reconciling visual field defects and retinal nerve fibre layer asymmetric patterns in retrograde degeneration: an extended case series: retinal nerve fibre layer defects in retrograde degeneration. *Clin Exp Optom*. 2017;100:214–226.
46. Saionz EL, Busza A, Huxlin KR. Rehabilitation of visual perception in cortical blindness. In: Quartarone A, Ghilardi MF, Boller F, eds. *Handbook of Clinical Neurology*. Amsterdam: Elsevier; 2022:357–373.
47. Brown CE, Aminoltejari K, Erb H, Winship IR, Murphy TH. In vivo voltage-sensitive dye imaging in adult mice reveals that somatosensory maps lost to stroke are replaced over weeks by new structural and functional circuits with prolonged modes of activation within both the peri-infarct zone and distant sites. *J Neurosci*. 2009;29:1719–1734.
48. Brown CE, Li P, Boyd JD, Delaney KR, Murphy TH. Extensive turnover of dendritic spines and vascular remodeling in cortical tissues recovering from stroke. *J Neurosci*. 2007;27:4101–4109.
49. Harrison TC, Silasi G, Boyd JD, Murphy TH. Displacement of sensory maps and disorganization of motor cortex after targeted stroke in mice. *Stroke*. 2013;44:2300–2306.
50. Cavanaugh MR, Blanchard LM, McDermott M, Lam BL, Tamhankar M, Feldon SE. Efficacy of visual retraining in the hemianopic field after stroke: results of a randomized clinical trial. *Ophthalmology*. 2021;128:1091–1101.
51. Barbot A, Das A, Melnick MD, et al. Spared perilesional V1 activity underlies training-induced recovery of luminance detection sensitivity in cortically-blind patients. *Nat Commun*. 2021;12:6102.
52. Jansonius NM, Schiefer J, Nevalainen J, Paetzold J, Schiefer U. A mathematical model for describing the retinal nerve fiber bundle trajectories in the human eye: average course, variability, and influence of refraction, optic disc size and optic disc position. *Exp Eye Res*. 2012;105:70–78.
53. Cowey A, Alexander I, Stoerig P. Transneuronal retrograde degeneration of retinal ganglion cells and optic tract in hemianopic monkeys and humans. *Brain*. 2011;134:2149–2157.
54. Cowey A. Atrophy of retinal ganglion cells after removal of striate cortex in a rhesus monkey. *Perception*. 1974;3:257–260.
55. Johnson H, Cowey A. Transneuronal retrograde degeneration of retinal ganglion cells following restricted lesions of striate cortex in the monkey. *Exp Brain Res*. 2000;132:269–275.
56. Buren JMV. Trans-synaptic retrograde degeneration in the visual system of primates. *J Neurol Neurosurg Psychiatry*. 1963;26:402–409.

Investigative Ophthalmology & Visual Science

57. Davis BM, Guo L, Ravindran N, et al. Dynamic changes in cell size and corresponding cell fate after optic nerve injury. *Sci Rep*. 2020;10:21683.
58. Miettinen TP, Björklund M. Mitochondrial function and cell size: an allometric relationship. *Trends Cell Biol*. 2017;27:393–402.
59. Zhang X, Francis BA, Dastiridou A, et al. Longitudinal and cross-sectional analyses of age effects on retinal nerve fiber layer and ganglion cell complex thickness by Fourier-domain OCT. *Transl Vis Sci Technol*. 2016;5:1.
60. Saenz M, Fine I. Topographic organization of V1 projections through the corpus callosum in humans. *NeuroImage*. 2010;52:1224–1229.
61. El-Danaf RN, Huberman AD. Characteristic patterns of dendritic remodeling in early-stage glaucoma: evidence from genetically identified retinal ganglion cell types. *J Neurosci*. 2015;35:2329–2343.
62. Amato R, Catalani E, Dal Monte M, Cammalleri M, Cervia D, Casini G. Morpho-functional analysis of the early changes induced in retinal ganglion cells by the onset of diabetic retinopathy: the effects of a neuroprotective strategy. *Pharmacol Res*. 2022;185:106516.
63. Vecino E, Rodriguez FD, Ruzafa N, Pereiro X, Sharma SC. Glia–neuron interactions in the mammalian retina. *Prog Retin Eye Res*. 2016;51:1–40.

Investigative Ophthalmology & Visual Science